Role of Distributed Oxygen Addition and Product Removal in the Oxidative Coupling of Methane

Ioannis P. Androulakis and Sebastián C. Reyes
Corporate Research Laboratories, Exxon Research and Engineering Company, Annandale, NJ 08801

Modeling and optimization of C_2 hydrocarbon production via the oxidative coupling of methane (OCM) were studied. The model includes both homogeneous and heterogeneous reactions. Focusing on the use of detailed reaction networks, previously validated experimentally, and the critical role of oxygen in both methane activation and product degradation, this work systematically explores the use of controlled oxygen addition and product removal schemes that improve OCM performance. Based on a plug flow reactor that is divided into N_p stages, within which oxygen is added and/or products are removed, a rigorous optimization algorithm is developed that simultaneously maximizes C_2 yields and minimizes O_2 consumption. In the absence of catalyst and product removal, the C_2 yield is maximized at a fixed O_2/CH_4 ratio, but this maximum yield is independent of the form in which the oxygen is added (cofeed or staged). When a catalyst is added, the optimal C_2 yields show only gradual improvements with oxygen distribution because the benefits of the lower oxygen reaction order on the catalyst are adversely affected by concomitant surface degradation reactions. The largest yield improvements are obtained when the C_2 hydrocarbons are removed at each stage before they undergo oxidation reactions. Thus, when staged oxygen addition is combined with product removal in the presence of a catalyst, C_2 yields as high as 87% are achieved in about 20 stages. Such yield values are consistent with experiments in which continuous product separation schemes have been used.

Introduction

The oxidative coupling of methane (OCM) to higher hydrocarbons continues to be the focus of significant research in both industry and academia. The objective of these efforts is to devise a commercially viable process for utilizing abundant natural gas reserves that are remotely located around the world. A pioneering article by Keller and Bhasin (1982) showed that, albeit low yields, ethylene and ethane could be produced from methane and oxygen feeds at atmospheric pressure and at relatively high temperatures ($\sim$1,073 K). Their findings sparked a flurry of research activities that sought to improve these C_2 yields to economically attractive levels. Most of the early work focused on the synthesis of new catalysts that would favor the coupling reaction over the undesired oxidation of the C_2 products (Amenomiya et al., 1990; Lunsford, 1990; Krylov, 1993). Since then, several groups have been able to improve the yields observed by Keller and Bhasin (1982), but even the most active and selective catalysts have not yet achieved the targets required for economic feasibility (Kuo et al., 1989; Fox, 1993). Beside the issues of activity and selectivity, viable processes must also deal with the relatively high exothermicity of the reaction, thus complicating reactor design. Currently, there is a consensus that an inherent limitation of the OCM chemistry is the concomitant oxidation of the C_2 products (Labinger, 1988; Ekstrom et al., 1989; Mackie et al., 1990; Mackie, 1991). The oxygen attack typically results in yield-conversion trajectories that go through a maximum at some intermediate methane conversion. For typical cofeed operation in fixed-bed reactors, C_2 yields greater than about 30% have not been reported (Krylov, 1993). Thus, complementing the quest for new catalysts, the search for novel reactor configurations that seek to overcome the above limita-

Correspondence concerning this article should be addressed to S. C. Reyes.

tions has, more recently, received considerable attention. These approaches range from the selective removal of the C_2 products using various adsorption and membrane separation schemes (Omata et al., 1989; Tonkovich et al., 1993; Jiang et al., 1994; Hall and Myers, 1995; Cordi et al., 1997a,b) to controlled oxygen addition strategies that lessen product degradation (Choudhary et al., 1989; Schweer et al., 1994; Do et al., 1995). Some of these approaches have resulted in substantial improvements, reaching C_2 yields as high as 85% (Jiang et al., 1994). The lack of commercial implementations today, however, suggests that the cost involved in these alternative reactor-separator schemes likely outweighs the benefits and, thus, it establishes the need for even more active and selective catalysts and improved reactor designs.

This work describes a modeling and optimization study that systematically explores C_2 yield improvements by the controlled addition of oxygen and/or controlled removal of C_2 products, both in the presence or in the absence of an oxidative coupling catalyst. Although some related studies have been reported in the literature (Santamaria et al., 1992; Reyes et al., 1993; Cheng and Shuai, 1995; Coronas et al., 1997; Lu et al., 1997a,b), the present study offers a more rigorous and formal analysis of yield optimization during staged operation and makes use of detailed reaction mechanisms for both the gas-phase chemistry and the surface catalyzed steps. Other theoretical studies of C_2 yield optimization on a simulated countercurrent moving-bed chromatographic reactor (Kruglov et al., 1996) and in a fixed-bed reactor that includes the mass and heat control along its distance (Rojnuckarin et al., 1996) have also been recently published and have merits of their own.

The details of the homogeneous and heterogeneous reaction mechanisms, on which the simulation and optimization results are based, are discussed first. This work emphasizes the use of reliable gaseous and catalytic networks that have been validated against experiments and which have been previously found suitable for describing compositional effects at typical methane coupling conditions of pressure and temperature. Thermodynamic calculations and reaction kinetic simulations are used first to illustrate some key features of the OCM chemistry, particularly regarding the issues of ethylene and ethane oxidation, pyrolysis under oxygen-depleted conditions, the role of the catalyst on methane activation and surface oxidation, and the need of product removal for achieving high C_2 yields. The gaseous and catalytic reaction networks are then embedded into rigorous optimization algorithms that seek to maximize the C_2 yields under a variety of situations that include, independently or simultaneously, the effects of catalyst addition, staged oxygen distribution, and staged product removal.

The most salient results of this modeling and optimization study can be summarized as follows. In the absence of catalyst and of product removal, the optimization algorithm identifies that C_2 yields are maximized when an optimal amount of O_2 is used; this maximum yield value, however, is independent of whether the oxygen is cofed or distributed along the reactor in multiple stages. Under oxygen co-feed operation, the addition of catalyst decreases the reaction time markedly but increases the yields only moderately. Staged oxygen addition in the presence of a catalyst brings only small yield improvements, because the concurrent surface oxidation reactions compete strongly with the methane activation step throughout the range of oxygen partial pressures. The optimization results indicate that, by far, the largest C_2 yield improvements occur under the staged product removal schemes. Thus, when product removal is complemented by staged oxygen addition in the presence of a catalyst, yields of nearly 87% are achieved in 20 stages.

Homogeneous and Heterogeneous Reaction Networks

Homogeneous reactions

The gas-phase reaction mechanism used in this study is taken from a recent publication by Mims et al. (1994). It involves an extensive set of free radical reactions that, in conjunction with isotope experiments, were successfully used to interpret mechanistic details of ethylene secondary reactions at OCM conditions (Mims et al., 1994). The network consists of 115 species that participate in 447 reversible reactions. An important feature of the network, which is largely responsible for the numerous species and reactions, is the inclusion of detailed reaction pathways for C_3 and C_4 hydrocarbons. There are also some higher molecular weight species such as 1,3-cyclopentadiene and benzene, as well as 1,3-cyclopentadienyl, 4-cyclopentenyl, and 1,4-pentadienyl radicals. Accordingly, this network has only limited capabilities for describing molecular weight growth and care is taken here of not using it under oxygen-depleted conditions. Also, in order to avoid errors in incorporating such large network into our computer algorithms, an original version was provided to us by the developers of the network (Mims et al., 1994). This version contains the network in Chemkin-II format and is complemented by the thermodynamic database that is required to calculate the reverse rate constants and the physico-chemical properties of the reaction mixture. Finally, it is noted that, despite the extensive computations involved in the optimization calculations, the accuracy of the reaction mechanism was not compromised by altering the network in any way.

Heterogeneous reactions

The catalytic OCM kinetics are taken from a very recent work by Colussi and Amorebieta (1997), who carried out a theoretical and experimental investigation of the maximum C_2 yields achievable in a continuous flow reactor containing a Sm_2O_3 catalyst. In line with the purposes of the present study, their catalyst system was chosen to illustrate the role of the surface-catalyzed steps on the overall C_2 yields under controlled oxygen environments. Colussi and Amorebieta's mechanism explicitly addresses the issue of oxygen reaction order; it has necessary details to be useful in computer modeling, and it has been validated against their own experimental data. Clearly, however, the methodology developed here can also be used in conjunction with other catalyst systems for which reaction mechanisms have been developed (such as Hoebink et al., 1994; Andrianova et al., 1996; Pannek and Mleczco, 1996; Wolf et al., 1998).

In their analysis of the OCM chemistry, Colussi and Amorebieta (1997) complemented the surface-catalyzed steps with a reduced set of seven free radical reactions. These gas-phase reactions are instead replaced here with the more de-

tailed homogeneous reaction mechanism described in the previous section. The carbon oxide species (CO_x) appearing in their original mechanism have also been explicitly separated into CO and CO_2 according to the stoichiometrics shown below (see also Amorebieta and Colussi, 1995, 1996)

$$CH_4 + 1/2\ O_{s1} \xrightarrow{k_1} CH_3 + 1/2\ H_2O,\ \ O_2(g) \overset{K_I}{\longleftrightarrow} 2O_{s1} \quad (1)$$

$$CH_3 + 5/2\ O_{s2} \xrightarrow{k_2} CO + 3/2\ H_2O,\ \ O_2(g) \overset{K_{II}}{\longleftrightarrow} 2O_{s2} \quad (2)$$

$$C_2H_6 + 1/2\ O_{s3} \xrightarrow{k_3} C_2H_5 + 1/2\ H_2O,\ \ O_2(g) \overset{K_{III}}{\longleftrightarrow} 2O_{s3} \quad (3)$$

$$C_2H_4 + 5\ O_{s4} \xrightarrow{k_4} CO + CO_2 + 2\ H_2O,\ \ O_2(g) \overset{K_{IV}}{\longleftrightarrow} 2O_{s4} \quad (4)$$

The numerical values of the kinetic constants ks and the equilibrium constants Ks can be found in their original publication (Colussi and Amorebieta, 1997). The above reactions show that, in addition to the desired methyl radical generation at the catalyst surface, degradative reactions also take place. Thus, ethane is converted to ethyl radicals and methyl radicals, and ethylene are degraded to carbon oxides and water. According to their experimental data, the rate of the above reactions could be adequately described by the following rate expression

$$-\frac{d[X]}{dt} = \frac{k_x[X]}{1 + K_x^{-1/2}[O_2]^{-1/2}},$$

$$[X] = [CH_4, CH_3, C_2H_6, C_2H_4] \quad (5)$$

At typical OCM conditions of pressure and temperature, these rate expressions become independent of oxygen concentration and therefore suggest that OCM performance can be improved by controlled oxygen strategies. As shown later, however, the benefits of oxygen staging are severely curtailed by the detrimental reactions (Eqs. 2–4), which oxidize the methyl radicals and also the ethane and ethylene products.

Modeling and Optimization

Modeling

This section summarizes the modeling equations that describe the evolution of reactants and products along the reactor length. Since the calculations are specialized to constant pressure and isothermal operation, no heat balance is required. Using mass fractions, the material balance equations can be written as

$$\frac{d\chi_i}{dz} = \frac{\epsilon}{\rho_0 u_o} \cdot \sum_{j=1}^{G} R_{ij} + \frac{(1-\epsilon)}{\rho_0 u_o} \cdot \left(a_p \cdot \sum_{k=1}^{S} L_{ik} + \theta \cdot \sum_{j=1}^{G} R_{ij} \right),$$

$$\chi_i(0) = \chi_{i0}, \quad i = 1, \ldots, N \quad (6)$$

In these equations, z is the axial reactor position, χ_i is the mass fraction of species i, ρ_0 is the inlet mass density, u_0 is the inlet interstitial velocity, a_p is the catalyst internal surface area per unit volume, and ϵ and θ are the reactor and particle void fractions, respectively. R_{ij} and L_{ik} are the rates of reaction (mass units) of the ith species in reactions j (gas phase) and k (catalyst surface), respectively. As described previously, the total number of species are $N = 115$, the total number of reactions in the gas phase are $G = 447$ and in the catalyst surface are $S = 4$. The time taken to the reacting mixture to reach the axial position z is obtained by integrating the following equation

$$\frac{dt}{dz} = \frac{\rho}{\rho_0 u_o}, \qquad t(0) = 0 \quad (7)$$

Thus, by specifying pressure temperature, and inlet mass fractions, the integration of Eqs. 6 and 7 determine the elapsed time and the species concentration along the reactor distance. The Chemkin-II package (Kee et al., 1990) is used to calculate the rates of reaction and the properties of the reacting mixture. The following numerical values are used in all the calculations described here: $\epsilon = 0.4$, $\theta = 0.4$, $u_0 = 100$ cm/s, and $a_p = 2 \cdot 10^5$ cm^2/cm^3.

Optimization

This section formulates a mathematical optimization problem that seeks to maximize the overall production of C_2 hydrocarbons in a plug-flow reactor having N_p discrete stages along its length. As shown in Figure 1, such an arrangement corresponds to a series of sequentially-connected subreactors containing injection and ejection points. The r_i and p_i represent oxygen addition and product removal points at the ith stage, respectively. The length of each subreactor is x_i and its numerical value is not known *a priori*. As shown later, the x_is are determined from the solution of the optimization problem itself. Thus, in addition to the integration of the species concentration with distance, material balances are applied to each subreactor to account for the mass added or removed.

The methane feed is always added to the first subreactor and the objective of the optimization problem is to maximize the yield of C_2 products accumulated throughout all the stages

$$Y = \sum_{i=1}^{N_p} \sum_{s \in S} \alpha_s Y_s(x_i), \quad S = \{C_2H_2, C_2H_4, C_2H_6\} \quad (8)$$

Y represents the combined yield of ethane, ethylene, and acetylene, and is defined in the usual manner as the product of selectivity and conversion. The coefficients α make it pos-

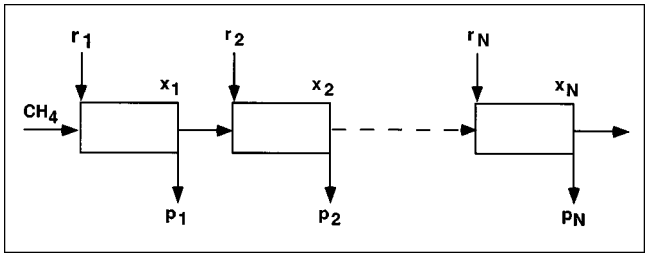

Figure 1. Distributed injection/ejection reactor configuration used in the optimization of C_2 yields.

sible to target final products with preferred proportions of C_2H_6, C_2H_4, and C_2H_2. Given a methane feed and a number of event points, the optimization problem consists of finding: (a) the amount of oxygen injected at each location (if any); (b) the amount of product removed at each location (if any); and (c) the location of the event point. Since the objective of the optimization is also to minimize the total amount of oxygen that is fed to the reactor, the entire mathematical problem is formulated as follows

$$\max_{x,r,p} \ \omega_1 \sum_{i=1}^{N_p} \sum_{s \in S} \alpha_s Y(x_i) + \omega_2 \sum_{i=1}^{N_p} r_i \tag{9}$$

subject to

$$\frac{d\chi_i}{dz} = f(\chi, x, r, p), \qquad i = 1, \ldots, N \quad 0 < z < x_i \tag{10}$$

$$\underline{R} \le \sum_{i=1}^{N_p} r_i \le \overline{R} \tag{11}$$

$$r_i(r_i - \underline{R}) \ge 0, \qquad i = 1, \ldots, N_p \tag{12}$$

$$p_i(p_i - \underline{P}) \ge 0, \qquad i = 1, \ldots, N_p \tag{13}$$

$$r_i \le Cx_i, \qquad i = 1, \ldots, N_p \tag{14}$$

$$p_i \le Cx_i, \qquad i = 1, \ldots, N_p \tag{15}$$

$$X_{O_2}(x_i) \le X_{O_2}^{\max} \tag{16}$$

The first constraint simply describes the compositional changes of each species within each subreactor (that is, the material balance Eq. 6). The second constraint limits the total amount of oxygen within some prespecified lower and upper bounds. The third and fourth constraints ensure that, unless a minimum amount is injected/ejected, the event does not take place. The fifth and sixth constraints impose that no mass should be injected and/or ejected if no event point is identified ($C \gg 1$). The last constraint establishes that a new stage is defined only after a predetermined O_2 conversion level is achieved in the prior stage. Unless specified otherwise, this maximum O_2 conversion value is taken here as 99%.

Notice that instead of posing a multiobjective optimization problem to maximize the C_2 yield, while simultaneously minimizing the oxygen consumption, an objective function based on weighting factors has been chosen. For suitable choices of the weighting factors ω_1 ($=1$) and ω_2 ($=-1$), such a formulation was found to be adequate to the objectives of this work. Although not further addressed here, the role of ω_1 and ω_2 becomes important when cost considerations are included in the objective function (that is, the difference between the value of products minus the cost of oxygen). Also, the number of stages N_p is used as a parameter instead of an optimized variable. This was prompted by the difficulty of penalizing the monotonic increase in the number of stages in any other way other than on economic grounds. This is outside the scope of the present study. Economic penalties are important in this problem since product yields increase gradually with the number of stages.

Numerically, the above optimization problem is solved using the NPSOL variant of the NAG Fortran Library. Integration is carried out with either DVODE or DDASSL (Brenan et al., 1996), but any other integration package able to handle stiff, nonlinear, ODE's should suffice. First-order derivatives are computed numerically. The approach is fairly straightforward and well-suited to the purposes of the present calculations since computational efficiency is not the key target.

Equations 9–16 represent a general mathematical optimization problem that is solved here for a number of special cases that independently or simultaneously quantify the effects of oxygen addition and of product removal on C_2 yields in the presence or absence of a catalyst. Thus, with or without catalyst, the following cases are analyzed in the next section: (1) staged oxygen addition; (2) staged product removal; and (3) staged oxygen addition in combination with staged product removal. It is noted that, in all the cases examined here, the existence of multiple local minima cannot be ruled out. The main focus of the calculations was to obtain a meaningful set of results that demonstrated the advantages of the staged oxygen addition and of the product removal strategies even if these results could be associated with local minima.

Results and Discussion

Simulation

Figure 2 shows a typical gas-phase yield-conversion trajectory in a co-feed reactor at 101.3 kPa and 1,073.15 K. The integration was carried out up to an oxygen conversion of 99.9% to probe the response of the network at low oxygen concentrations. The residence time required to achieve the overall maximum yield is about 0.5 s. Consistent with the early experimental observations of Keller and Bhasin (1982), the dominant coupling products are ethylene and ethane. Small amounts of acetylene form only at very high oxygen conversion levels, where dehydrogenation reactions of ethane and ethylene become important. The individual yield trajectories

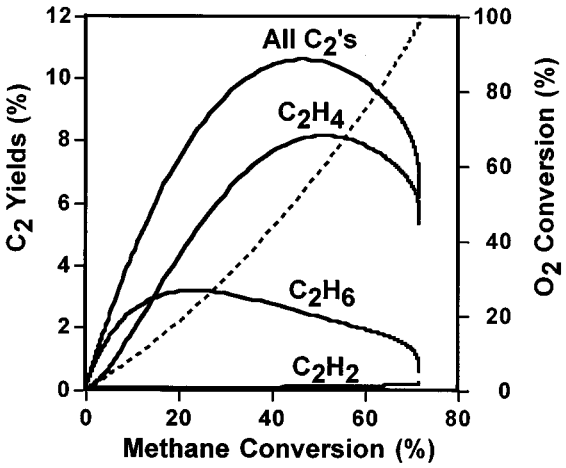

Figure 2. Ethane, ethylene, and acetylene yields and oxygen conversion (– – –) as a function of methane conversion.

$O_2/CH_4 = 1$, 1,073.15 K, 101.3 kPa, no catalyst.

are clearly consistent with a consecutive reaction scheme that sequentially converts $C_2H_6 \rightarrow C_2H_4 \rightarrow C_2H_2$. The non-zero slope for ethane formation at low methane conversion confirms that ethane is the primary product of the coupling reaction.

Consistent with the expected behavior of purely homogeneous reactions, the overall C_2 yield goes through a maximum of 10.56% at an intermediate methane conversion of 46.8%. Beyond this conversion value, the overall yield declines due to oxidation reactions of the C_2 products. These oxidation reactions become important throughout the methane conversion region where both the oxygen partial pressure and the concentration of C_2 hydrocarbons are significant. Ultimately, as oxygen becomes severely depleted, other mechanisms of C_2 yield degradation take place. They correspond to kinetically-slower pyrolysis reactions that lead to the formation of higher molecular weight products (C_2^+) and also to reforming reactions of methane with CO_2 and H_2O to form additional CO and H_2. This region of high oxygen depletion is not of interest to the OCM chemistry and is purposely avoided during the present optimization calculations, because the homogeneous mechanism cannot adequately describe the molecular weight growth processes that take place as the system progresses towards thermodynamic equilibrium. More suitable reaction networks that specifically address these pyrolysis reactions are available in the literature (Dean, 1990).

Figure 3 shows gas-phase yield-conversion trajectories at various O_2/CH_4 feed ratios under co-feed operation. These results illustrate the key role of the oxygen partial pressure on methane activation, as well as on ethylene (and ethane) oxidation steps. This figure shows that an optimal O_2/CH_4 ratio exists in the range of 0.5 and 1. It also shows that for inlet O_2/CH_4 ratios lower than about 0.5, the decline in C_2 yield is principally associated with pyrolysis-like conditions: the sharp decline appears immediately after the point of maximum yield and, therefore, it suggests that most of the oxygen is used for the methane activation step. Also, reflecting the more selective chemistry that takes place at lower oxygen partial pressures, the slopes of the yield-conversion curves increase with decreasing oxygen in the feed. Thus, under co-feed operation, the trade-offs of oxygen control are clear: lesser amounts of oxygen induce more selective chemistry but limit the maximum attainable yields.

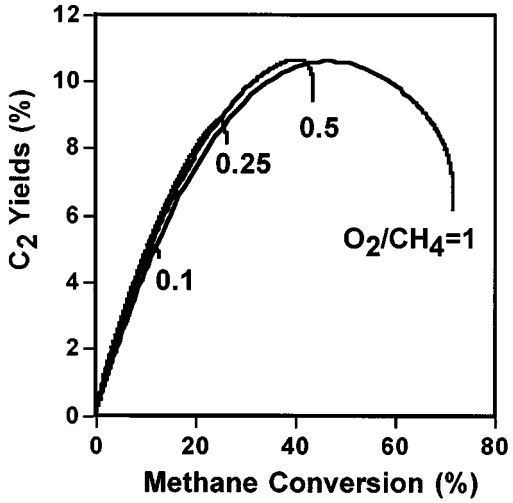

Figure 3. Gas phase C_2 yields as a function of methane conversion for various O_2/CH_4 ratios.
1,073.15 K, 101.3 kPa.

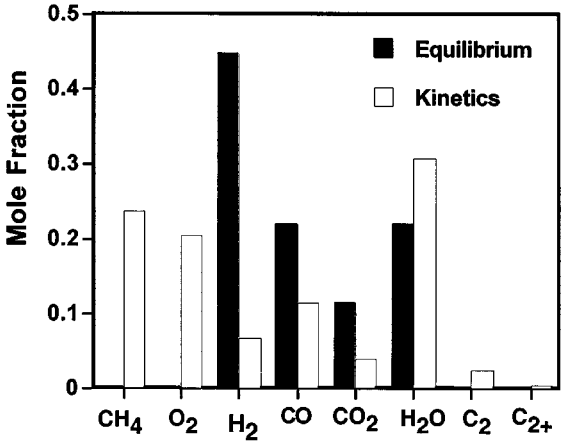

Figure 4. Comparison of mole fractions at thermodynamic equilibrium and from kinetic integration up to point of maximum C_2 yield.
$O_2/CH_4 = 1$, 1,073.15 K, 101.3 kPa.

Figure 4 compares the product distribution obtained at conditions of thermodynamic equilibrium with the corresponding values obtained by kinetic integration up to the point of maximum C_2 yield. The pressure, temperature, and inlet feed O_2/CH_4 ratio are the same as those described in Figure 2. This figure shows that at typical methane coupling conditions of pressure and temperature, the most abundant species at equilibrium are H_2, CO, H_2O, and CO_2. These species are also present in the kinetically-evolving mixture, but they are distributed in a much different proportion. The reacting mixture also has large amounts of unreacted methane and oxygen, small amounts of C_2s, and some C_2^+ products. These results illustrate that a key objective of the OCM chemistry is to exploit a kinetic trajectory that maximizes ethane and ethylene (reacting intermediates) that would be otherwise only minor components at conditions of thermodynamic equilibrium. This, therefore, suggests that the C_2 yields can be manipulated by controlling the surrounding oxygen partial pressure and/or by removing the C_2 products before oxidation and reforming reactions take place. The results of such strategies are discussed in the next section.

Finally, Figure 5 compares the C_2 yields obtained with and without a catalyst. It is seen that the catalyst brings about a measurable improvement in the maximum C_2 yield. The shape of the yield-conversion trajectory is largely maintained, except for the region of high oxygen conversion. This is simply due to the dominance of the catalytic reactions that control the reaction rates at times much shorter than those required for pyrolysis reactions. With the catalyst, the time taken to achieve the maximum yield is only 2 ms, which is significantly shorter than the 0.5 seconds required for the purely homogeneous reactions.

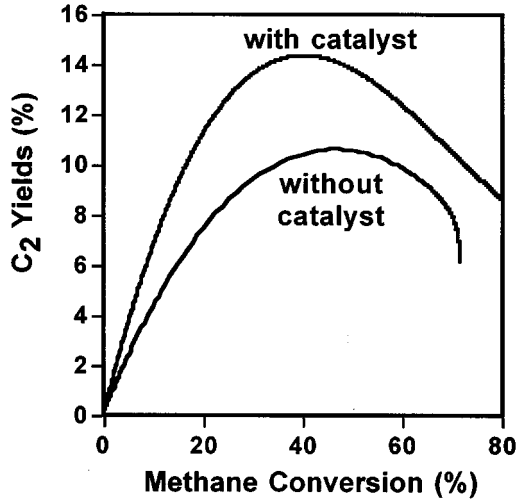

Figure 5. C_2 yields as a function of methane conversion in the presence and absence of a catalyst.

$O_2/CH_4 = 1$, 1,073.15 K, 101.3 kPa.

Optimization results

The optimization algorithm was first applied to the simplest of all cases contained within the general formulation: controlled addition of oxygen in the absence of a catalyst. The optimization sought to maximize the C_2 yield with the number stages N_p as a parameter. It was found that, irrespective of the value of N_p, the maximum C_2 yield reached a value of about 10.72% at an optimal O_2/CH_4 ratio of about 0.62. These values are consistent with the simulation results of the previous section that demonstrated a C_2 yield of 10.58% at $O_2/CH_4 = 1$ and suggested that, in a co-feed mode, additional improvements could be realized by controlling the O_2/CH_4 ratio between 0.5 and 1 (see Figure 3). Thus, in the absence of a catalyst, there is no incentive in staging the oxygen feed along the reactor length since a co-feed operation produces the same results.

The next level of calculations focused on maximizing the C_2 yields by distributing the oxygen along the reactor in the presence of a catalyst. The results are summarized in Table 1. They are reported in terms of the percentage of carbon in the products. Despite the low oxygen reaction order of the catalytic reactions compared to those of the gas phase, the optimization algorithm reveals only minor incentives for distributing the oxygen feed along the reactor length. The small increase with N_p is the result of a compensation effect between favorable and unfavorable surface-catalyzed processes. The catalytic methane activation that is favored over gas-phase oxidation at low oxygen partial pressures also favors the surface oxidation of methyl radicals, ethane, and ethylene. Thus, the small increment in methane conversion with the number of stages is nearly balanced by the selectivity losses to $CO + CO_2$ and C_{2+}. The optimal amount of oxygen is low and increases only slightly with the number of stages. It is kept low to minimize the concurrent gas-phase oxidation reactions, and it is responsible for the rather large amounts of C_{2+} products that form more readily at low oxygen concentrations.

Table 2 summarizes the optimal C_2 yields and oxygen requirements obtained for staged product removal in the absence of a catalyst and under oxygen co-feed conditions. In all product removal cases reported here, all the C_2H_6, C_2H_4, and C_2H_2 products are removed at each stage. This table shows that the C_2 yield increases markedly with the number of stages. Yields of nearly 50% are obtained for 20 stages. As N_p increases, sizable methane conversion increments occur without appreciable increases in carbon oxides and with decreasing C_{2+} formation. The removal of C_2 products limits their oxidation and their participation in molecular weight growth processes. It also allows the use of higher amounts of oxygen, that contribute proportionately more to methane activation than to product oxidation. The optimal amount of oxygen goes through a broad maximum that reflects a compromise between increased methane conversion and decreased product selectivity.

Table 3 summarizes the optimal C_2 yields and oxygen consumption obtained for staged oxygen addition and product

Table 2. Carbon Number Distribution as a Function of Number of Stages for a Plug-Flow Reactor Operating at 1,073.15 K*

N_p	CH_4	$CO + CO_2$	C_2	C_{2+}	O_2/CH_4
2	38.95	40.26	17.47	3.26	0.781
4	24.33	47.22	24.33	2.67	0.884
6	17.26	49.09	31.85	1.79	0.928
8	14.59	47.96	35.96	1.47	0.908
10	12.84	46.73	39.13	1.29	0.900
20	5.91	44.76	48.56	0.76	0.889

*Oxygen co-feed, staged product removal, no catalyst.

Table 1. Carbon Number Distribution as a Function of Number of Stages for a Plug-Flow Reactor Operating at 1,073.15 K*

N_p	CH_4	$CO + CO_2$	C_2	C_{2+}	O_2/CH_4
2	59.41	8.24	20.26	12.08	0.222
4	56.53	8.56	21.09	13.82	0.239
6	55.36	8.71	21.37	14.54	0.246
8	54.64	8.86	21.51	14.98	0.251
10	54.44	8.81	21.59	15.15	0.252
20	53.58	9.01	21.73	15.67	0.257

*Staged oxygen injection, no product removal, with catalyst.

Table 3. Carbon Number Distribution as a Function of Number of Stages for a Plug-Flow Reactor Operating at 1,073.15 K*

N_p	CH_4	$CO + CO_2$	C_2	C_{2+}	O_2/CH_4
2	38.47	39.49	17.78	4.23	0.820
4	19.29	51.03	26.46	3.21	0.993
6	17.00	46.83	32.98	3.17	1.010
8	11.99	46.73	38.29	2.97	1.010
10	8.98	45.99	42.12	2.89	1.038
20	3.91	40.06	53.68	2.33	0.963

*Staged oxygen injection, staged product removal, no catalyst.

Table 4. Carbon Number Distribution as a Function of Number of Stages for a Plug-Flow Reactor Operating at 1,073.15 K*

N_p	CH_4	$CO+CO_2$	C_2	C_{2+}	O_2/CH_4
2	44.38	12.61	31.98	11.07	0.310
4	24.59	15.91	49.69	9.79	0.406
6	15.33	15.79	60.94	7.92	0.432
8	10.39	14.59	68.62	6.38	0.432
10	7.26	13.47	74.11	5.14	0.428
20	2.06	8.62	87.21	2.09	0.379

*Staged oxygen injection, staged product removal, with catalyst.

removal in the absence of a catalyst. As in the previous case, the yield increases markedly with the number of stages. A one-to-one comparison of the results in Tables 2 and 3 shows that the additional effect of oxygen distribution lead to a further, though moderate, improvement in C_2 yields. The relatively larger amounts of oxygen allowed in this case have a more favorable effect on the methane conversion than on the formation of undesired carbon oxides. The longer residence times involved in the present case, due to the oxygen distribution, gives rise to slightly greater, though moderate, amounts of C_{2+} than in the previous case.

Table 4 summarizes the optimal C_2 yields and oxygen consumption obtained for staged oxygen addition and product removal in the presence of a catalyst. As expected, this case leads to the largest improvements in C_2 yields. The combination of catalyst and product removal is largely responsible for the marked improvements of this case compared to those discussed previously. Reflecting the very high methane conversion and very high selectivity at 20 stages, the yield reaches 87.2%. Also, consistent with the more selective chemistry under which this system operates, the total oxygen requirements are moderate and also go through a maximum that compensates the trade-offs of conversion and selectivity trends with increasing N_p.

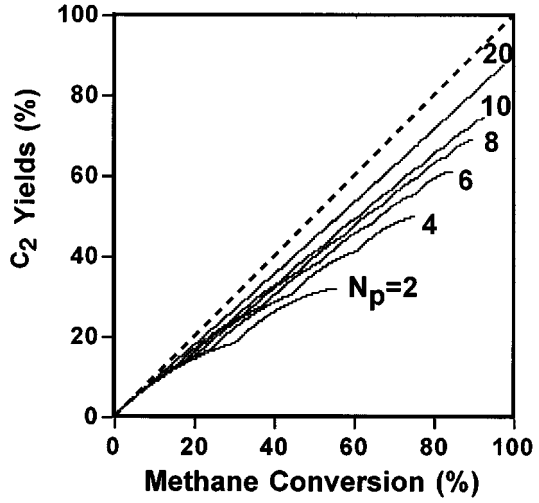

Figure 6. C_2 yield increments as a function of methane conversion for the conditions of Table 4.

Staged oxygen injection, staged product removal, with catalyst.

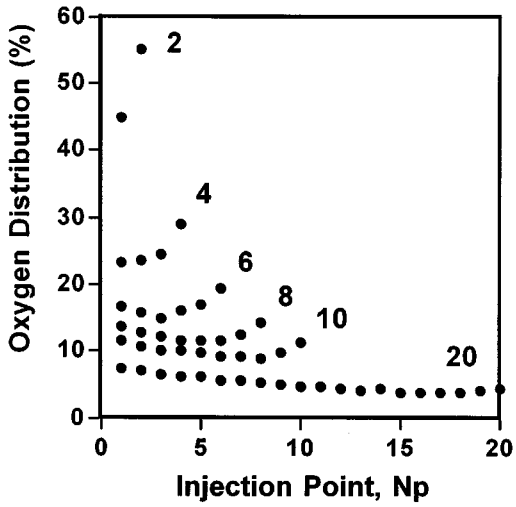

Figure 7. Percent of oxygen injected at each injection point for the conditions of Table 4.

Staged oxygen injection, staged product removal, with catalyst.

Figure 6 shows the stage-by-stage C_2 yield increments as a function of methane conversion for the conditions of Table 4. The yields increments are nearly uniform and, as N_p increases, follow trajectories that gradually approach the parity line of maximum selectivity. Under the present conditions, the C_2 yields increase monotonically with the number of stages. For N_p greater than about 20, this staged operation behaves like a dual function membrane that selectively permeates the oxygen in and separates the products out.

Complementing the results of Table 4 and Figure 6, Figure 7 displays how the oxygen is distributed among the various injection points. The relative amounts change as N_p increases. When N_p is low, the optimization algorithm determines that more oxygen should be added in the latter injection points. As N_p increases from 6 to 10, the relative amounts go through a shallow minimum. Finally, as N_p increases past about 10, the relative amounts become more uniform but still exhibit a slight decreasing trend. The nearly uniform injections that the algorithm determines for a large N_p further emphasizes the similarity of this discrete operation to a continuous membrane reactor.

Conclusions

Despite the extensive search for more active and selective catalysts that followed the pioneering work of Keller and Bhasin (1982), there is broad consensus today that co-feeding CH_4 and O_2 over an OCM catalyst leads to C_2 yields that do not meet the targets required for economic feasibility. Accordingly, as illustrated by the present work, some of the emphasis has shifted to engineering designs that take advantage of the OCM chemistry fundamentals, particularly regarding the preservation of the desired C_2 products and the minimization of detrimental oxidation pathways that occur on the catalyst surface and in the surrounding gas phase. Thus, based on a detailed modeling and optimization study, this work demonstrates that the maximum C_2 yields achievable in a

co-feed process can be significantly improved by controlling the addition of oxygen and the removal of C_2 products along multiple stages in a fixed-bed reactor. The focus of this analysis is on potential C_2 yield improvements based on chemistry fundamentals and, therefore, cost or implementation issues are not addressed. The results are based on realistic homogeneous and heterogeneous chemical mechanisms that have been previously verified experimentally and which describe well compositional effects at typical conditions of pressure and temperature. In all cases involving oxygen distribution, the algorithms prescribe the optimal amounts of oxygen added at each stage and their location along the reactor.

The combination of catalyst and oxygen control without product removal leads to only moderate yield improvements because, despite the significant lowering of gas-phase oxidation rates at low oxygen partial pressures, significant surface oxidation reactions occur in parallel with the production of methyl radicals. Thus, the expected advantages of a low oxygen reaction order in the catalyst are negated by the concurrent nonselective surface oxidation steps. Although this conclusion is strictly valid for the Sm_2O_3 catalyst considered in the present study, it appears to be applicable to OCM catalyst systems in general. As expected, the largest C_2 yield improvements are realized when the products are removed from the reactor, thereby preventing their oxidation in either the catalyst or the surrounding gas phase. Thus, when staged oxygen addition is combined with staged product removal over a catalyst, C_2 yields as high as 87% are obtained in 20 stages. These yield values are consistent with those obtained by Cordi et al. (1997a,b) and by Jiang et al. (1994) through the use of a membrane reactor and recycle reactor-separator, respectively, and, therefore, provide some support for the validity of our optimization algorithms and the underlying catalytic and gaseous chemistry on which the results are based.

Notation

α_s = weight factors in Eq. 8
C = large positive constant
k_i = kinetic constants of surface reactions
K_i = equilibrium constants for adsorbed oxygen
$\underline{P}$ = lower bound for product removal
$\underline{R}$ = lower bound for oxygen amount
$\overline{R}$ = upper bound for oxygen amount
t = time
x_i = location of stage i
X = species composition
$\chi_{O_2}^{max}$ = maximum O_2 conversion within a stage

Literature Cited

Amenomiya, Y., V. I. Birss, M. Goledzinowski, J. Galuszka, and A. R. Sanger, ''Conversion of Methane by Oxidative Coupling,'' *Catal. Rev.-Sci. Eng.*, **32**, 163 (1990).

Amorebieta, V. T., and A. J. Colussi, ''Kinetics and Mechanism of the Heterogeneous Oxidation of Methyl Radicals on Samarium (III) Oxide. Implications for the Oxidative Coupling of Methane,'' *J. Am. Chem. Soc.*, **117**, 3856 (1995).

Amorebieta, V. T., and A. J. Colussi, ''Kinetics and Mechanism of the Heterogeneous Oxidation of Ethane and Ethylene on Samarium (III) Oxide,'' *J. Am. Chem. Soc.*, **118**, 10326 (1996).

Andrianova, Z. S., A. N. Ivanova, P. E. Matkovskii, and G. P. Startseva, ''Mathematical Modeling of Heterogeneous Steps of Oxidative Coupling of Methane to Ethane and Ethylene. Kinetics and Catalysis,'' **37**, 246 (1996).

Baerns, M., and W. Hinsen, ''Process for the Production of Ethane and/or Ethylene from Methane,'' U.S. Patent 4,608,449 (1986).

Brenan, K. E., S. L. Campbell, and L. R. Petzold, *Numerical Solution of Initial-Value Problems in Differential-Algebraic Equations*, SIAM Series in Applied Mathematics, SIAM, Philadelphia (1996).

Cheng, S., and X. Shuai, ''Simulation of a Catalytic Membrane Reactor for Oxidative Coupling of Methane,'' *AIChE J.*, **41**, 1598 (1995).

Choudhary, V. R., S. T. Chaudhari, A. M. Rajput, and V. H. Rane, ''Beneficial Effect of Oxygen Distribution on Methane Conversion and C_2-Selectivity in Oxidative Coupling of Methane to C_2-Hydrocarbons over Lanthanum-Promoted Magnesium Oxide,'' *J. Chem. Soc. Chem. Commun.*, **20**, 1526 (1989).

Colussi, A. J., and V. T. Amorebieta, ''Optimum Yield of the Purely Heterogeneous Dimerization of Methane,'' *J. Catal.*, **169**, 301 (1997).

Cordi, E. M., P. Qui, J. H. Lunsford, and M. P. Rosynek, ''Development of an Integrated System for the Production of Olefins from the Oxidative Coupling of Methane,'' presented at the 15th North American Meeting of the Catalysis Society, Chicago, IL (May 18–22, 1997a).

Cordi, E. M., S. Pak, M. P. Rosynek, and J. H. Lunsford, ''Steady-State Production of Olefins in High Yields during the Oxidative Coupling of Methane: Utilization of a Membrane Contactor,'' *Appl. Catal.*, **155**, L1 (1997b).

Coronas, J., A. Gonzalo, D. Lafarga, and M. Menendez, ''Effect of the Membrane Activity on the Performance of a Catalytic Membrane Reactor,'' *AIChE J.*, **43**, 3095 (1997).

Dean, A. M., ''Detailed Kinetic Modeling of Autocatalysis in Methane Pyrolysis,'' *J. Phys. Chem.*, **94**, 1432 (1990).

Do, K. T., J. H. Edwards, and R. J. Tyler, ''The Catalytic Oxidative Coupling of Methane: I. Comparison of Experimental Performance Data from Various Types of Reactor,'' *Can. J. Chem. Eng.*, **73**, 327 (1995).

Ekstrom, A., J. A. Lapszewicz, and I. Campbell, ''Origins of the Low Limits in the Higher Hydrocarbon Yields in the Oxidative Coupling of Methane,'' *Appl. Catal.*, **56**, L29 (1989).

Fox, J. M., ''The Different Catalytic Routes for Methane Valorization: An Assessment of Processes for Liquid Fuels,'' *Catal. Rev.-Sci. Eng.*, **35**, 169 (1993).

Hall, R. B., and G. R. Myers, *Effects of Product Separation on the Kinetics and Selectivity of Oxidative Coupling. Methane and Alkane Conversion Chemistry*, M. M. Bhasin and D. W. Slocum, eds., Plenum Press, New York, p. 123 (1995).

Hoebink, J. H. B. J., P. M. Couwenberg, and G. M. Marin, ''Fixed Bed Reactor Design for Gas Phase Chain Reactions Catalysed by Solids: The Oxidative Coupling of Methane,'' *Chem. Eng. Sci.*, **49**, 5453 (1994).

Jiang, Y., I. V. Yentekakis, and C. G. Vayenas, ''Methane to Ethylene with 85% Yield in a Gas Recycle Electrocatalytic Reactor-Separator,'' *Science*, **264**, 1563 (1994).

Kee, R. J., F. M. Rupley, and J. A. Miller, ''Chemkin-II: A Fortran Chemical Kinetics Package for the Analysis of Gas-Phase Chemical Kinetics,'' Sandia National Laboratories, Report SAND89-8009 (1990).

Keller, G. E., and M. M. Bhasin, ''Synthesis of Ethylene via Oxidative Coupling of Methane. I. Determination of Active Catalysts,'' *J. Catal.*, **73**, 9 (1982).

Kruglov, A. V., M. C. Bjorklund, and R. W. Carr, ''Optimization of the Simulated Countercurrent Moving-Bed Chromatographic Reactor for the Oxidative Coupling of Methane,'' *Chem. Eng. Sci.*, **51**, 2945 (1996).

Krylov, O. V., ''Catalytic Reactions of Partial Methane Oxidation,'' *Catal. Today*, **18**, 209 (1993).

Kuo, J. C. W., C. T. Kresge, and R. E. Palermo, ''Evaluation of Direct Methane Conversion to Higher Hydrocarbons and Oxygenates,'' *Catal. Today*, **4**, 463 (1989).

Labinger, J. A., ''Oxidative Coupling of Methane: An Inherent Limit to Selectivity?,'' *Catal. Letters*, **1**, 371 (1988).

Lu, Y., A. G. Dixon, W. R. Moser, and Y. M. Ma, ''Analysis and Optimization of Cross-Flow Reactors with Distributed Reactant Feed and Product Removal,'' *Catal. Today*, **35**, 443 (1997a).

Lu, Y., A. G. Dixon, W. R. Moser, and Y. H. Ma, ''Analysis and

Optimization of Cross Flow Reactors for Oxidative Coupling of Methane,'' *Ind. Eng. Chem. Res.*, **36**, 559 (1997b).
Lunsford, J. H., ''The Catalytic Conversion of Methane to Higher Hydrocarbons,'' *Catal. Today*, **6**, 235 (1990).
Mackie, J. C., J. G. Smith, P. N. Nelson, and R. J. Tyler, ''Inhibition of C_2 Oxidation by Methane Under Oxidative Coupling Conditions,'' *Energy and Fuels*, **4**, 277 (1990).
Mackie, J. C., ''Partial Oxidation of Methane: The Role of the Gas Phase Reactions,'' *Catal. Rev.-Sci. Eng.*, **33**, 169 (1991).
Mims, C. A., R. Mauti, A. M. Dean, and K. D. Rose, ''Radical Chemistry in Methane Oxidative Coupling: Tracing Ethylene Secondary Reactions with Computer Models and Isotopes,'' *J. Phys. Chem.*, **98**, 13357 (1994).
NAG Fortran Library, *The Numerical Algorithms Group Limited, Mark* 17, 1st ed. (Sept. 1995).
Omata, K., S. Hashimoto, H. Tominaga, and K. Fujimoto, ''Oxidative Coupling of Methane Using a Membrane Reactor,'' *Appl. Catal.*, **52**, L1 (1989).
Pannek, U., and L. Mleczko, ''Comprehensive Model of Oxidative Coupling of Methane in a Fluidized-Bed Reactor,'' *Chem. Eng. Sci.*, **51**, 3575 (1996).
Reyes, S. C., E. Iglesia, and C. P. Kelkar, ''Kinetic-Transport Models of Bimodal Reaction Sequences—I. Homogeneous and Heterogeneous Pathways in Oxidative Coupling of Methane,'' *Chem. Eng. Sci.*, **48**, 2643 (1993).
Rojnuckarin, A., C. A. Floudas, H. Rabitz, and R. A. Yetter, ''Methane Conversion to Ethylene and Acetylene,'' *Ind. Eng. Chem. Res.*, **35**, 683 (1996).
Santamaria, J., M. Menendez, J. A. Peña, and J. I. Barahona, ''Methane Oxidative Coupling in Fixed Bed Catalytic Reactors with a Distributed Oxygen Feed. A Simulation Study,'' *Catal. Today*, **13**, 353 (1992).
Schweer, D., L. Mleczko, and M. Baerns, ''OCM in a Fixed-Bed Reactor: Limits and Perspectives,'' *Catal. Today*, **21**, 357 (1994).
Tonkovich, A. L., R. W. Car, and R. Aris, ''Enhanced C_2 Yields from Methane Oxidative Coupling by Means of a Separative Reactor,'' *Science*, **262**, 221 (1994).
Wolf, D., M. Slinko, E. Kurkina, and M. Baerns, ''Kinetic Simulations of Surface Processes of the Oxidative Coupling of Methane over a Basic Oxide Catalyst,'' *Appl. Catal. A: General*, **166**, 47 (1998).

Manuscript received Nov. 3, 1998, and revision received Feb. 16, 1999.